Final report on the grant number PD123790

The report list the series of studies that have been completed throughout the period. All studies are discussed in detail separately including theoretical background methods and results including their dissemination. All data published from the research grant is available at OSF (https://osf.io/).

1. Temporal expectations based on statistical learning modulate coupling within a distributed network of brain areas.

1.1. Background

A large body of evidence suggests that the adult human brain tracks temporal/sequential regularities in the auditory input, establishing and continuously refining internal models that generate predictions for future events (Friston & Kiebel, 2009; Rubin, Ulanovsky, Nelken, & Tishby, 2016; Winkler, Denham, & Nelken, 2009; McDermott, Schemitsch, & Simoncelli, 2013; Paavilainen et al., 2013; Saffran, Johnson, Aslin, & Newport, 1999). The ability to continuously form and update predictions about our current context, for instance, to anticipate the timing of an event, is a fundamental cognitive operation for behavior optimization and preservation of resources. Optimal timing implies a form of predictive adaptation to the temporal structure of events, to circumvent exclusively reactive behavior (Kotz et al.,2014). It is established, that temporal context can shape perceptual processing: Different forms of dynamic Attending (future-oriented or analytic), can affect the estimate of events, based on their structural predictability Stefanics et al 2010, Auksztulewicz et al 2017, Jones et al., 1989). However, the neural mechanisms and large-scale neural networks that underlie the learning of temporal context have not yet been identified. The aim of the study is to understand how is behavior governed in a temporal context: Is the processing of behaviorally relevant stimuli facilitated by probability-based confidence of anticipation? Does functional brain connectivity mediate the effects of expectation on the processing of behaviorally relevant stimuli?

1.2. Methods

Participants, procedure, and stimuli: Twenty healthy young adults participated in the study (10 females; mean age: 22.4 ± 2,35). Subjects are asked to press a button upon target detection Participants performed the auditory target detection task. They were instructed to detect the target as soon as they can by button press. There was always a cue preceding the target. The interval between the cue and the target (ISI) was either 1200 or 2400 ms (short vs long ISI).
Two types of Cue (tones of distinct frequencies: 1048 and 1818 Hz; 100 ms duration; 10 ms rise/fall times) were used to predict the probability (20% and 80%; 50% and 50%) of the target stimulus (1876 Hz; 100 ms duration; 10 ms rise/fall times) to appear at either of two fixed time points (early target at 1300 ms and late target at 2600 ms). Cue manipulation yielded two conditions: predictable (80% short ISI, early target, 20% long ISI, late target) unpredictable (50% short ISI, early target, 50% long ISI, late target).

Behavioral data analysis: Repeated measures ANOVA was calculated on reaction time data using within-subject predictability condition (predictable vs. unpredictable) and target type (early vs. late)

EEG data analysis: Epochs from the raw recording of 64-channel scalp EEG extend from 1000 ms before and 4000 ms after the time-locking event. Artifact removal was performed with ICA and an automatic threshold detection (+/- 100 µV) procedure. EEG source localization using sLORETA was based on the combination of individual MRIs and adjusted default electrode positions. Directed functional connectivity between brain regions was measured by Granger causality estimates for trial averages of each condition. Granger values are given over a window length of 250 ms. Significant contrasts of predictable vs. unpredictable were deemed based on cluster-based permutation tests.

1.3. Results

In this experiment, we measured the effects of the predictive value of Cue stimuli on behavioral responses. We observed faster responses (lower RT) for predicted early targets relative to less predictable early targets while as expected there was a similar RT for late targets. Predictive cues elicited larger P2 amplitudes and lower N2 tendencies for early targets (see Fig 1.).

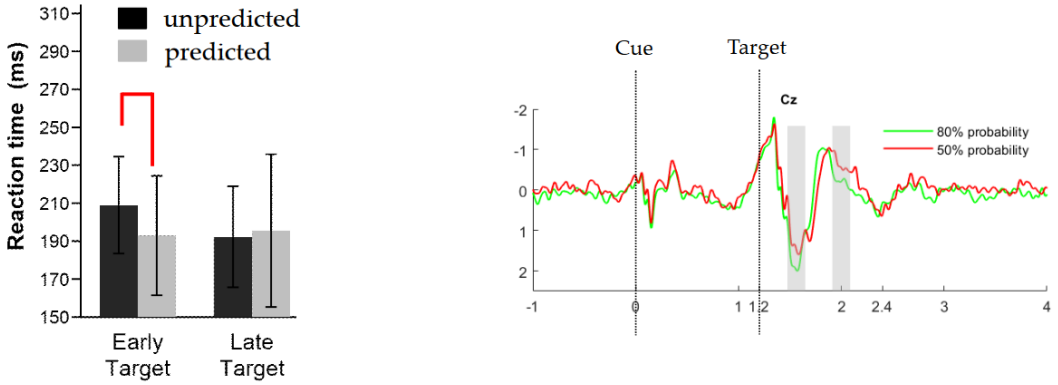

Fig 1. Behavioral results (left) and ERP responses (right) for predictable (green line) and unpredictable (red line) cues.

Figure 2 summarizes the results of the functional connectivity analysis. We observed higher connectivity for unpredicted stimuli compared to the predictable only in the left hemisphere from the precentral gyrus (PRE) towards the anterior cingulate gyrus (caudal, CAC) and also from the primary auditory cortex (Herschel gyrus -HG) to the precentral gyrus. Predictable cues induced stronger connectivity only in the right hemisphere from the primary auditory cortex (Herschel gyrus -HG) to the Inferior temporal gyrus (ITG), and also from the inferior temporal gyrus to the superior temporal gyrus (STG).

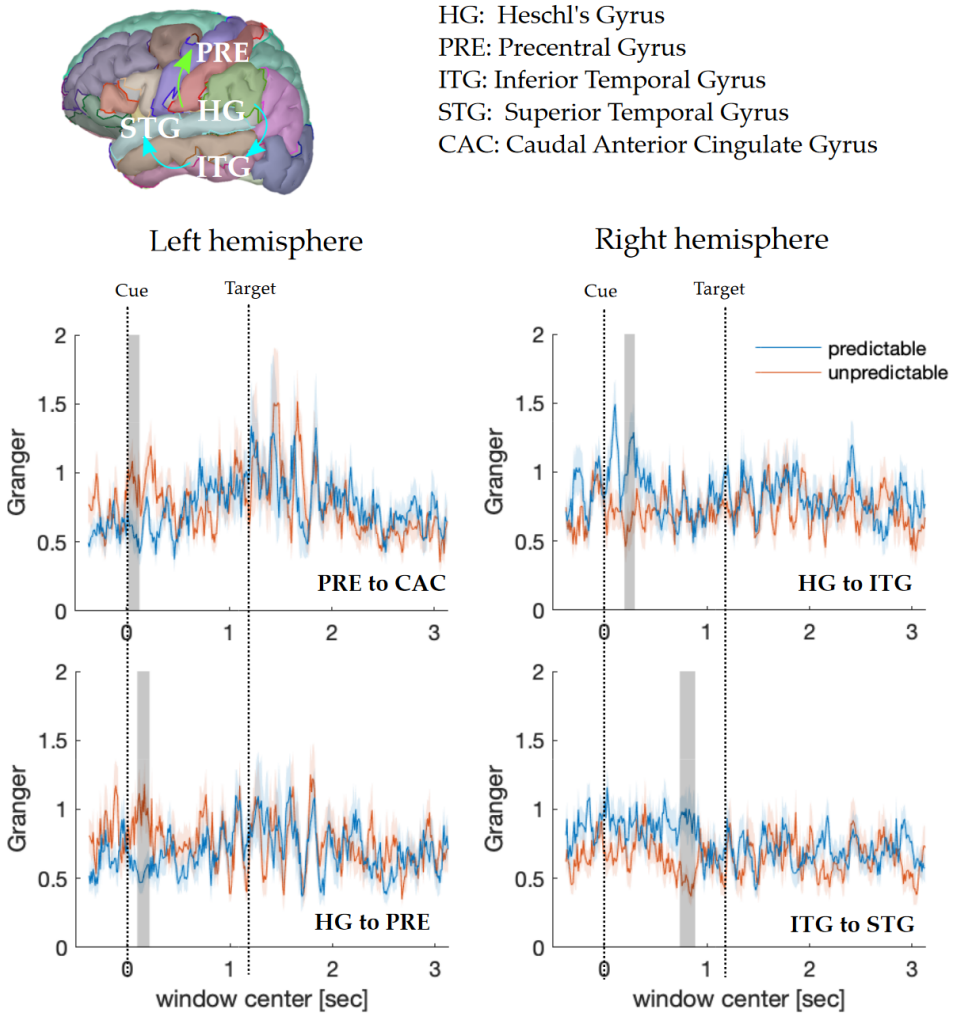

Fig2. Directed connectivity results. Top: Region of interests and their abbreviations. Bottom: Granger connectivity values as a function of time between ROIs on the left (left row) and the right (right row) hemisphere.

1.4. Discussion

The ability to anticipate the timing of an event is a fundamental cognitive operation for behavior optimization and the preservation of resources (Kotz et al.,2014, Arnal & Giraud, 2012)Auksztulewicz et al., 2017). Optimal timing implies a form of predictive adaptation to the temporal structure of events, to circumvent exclusively reactive behavior (ref). It is established, that temporal context can shape perceptual processing: Different forms of dynamic attending (future-oriented or analytic), can affect the estimate of events, based on their structural predictability (Kotz et al.,2014). The present study demonstrated that probability-based confidence accelerates behavioral and neural responses to target sounds (faster response to target event with neural enhancement on ERP responses). Neural enhancement of predicted event manifest in larger P2 and smaller N2 tendencies for early targets following predictive cues.

We suggest that the observed increased motor response preparation and control processes are linked to left-lateralized parietal-premotor action circuits (Coull, 2009). According to our results, the decrease in predictability was associated with decreased coupling within the

left-lateralized parietal-premotor action circuits. Right STG is associated with temporal expectancy based on temporal probability representations, ITG with temporal attention processes (Anderson, Sheinberg, 2008). In line, we found higher connectivity from HG to ITG and ITG to STG, for predicted stimuli. In conclusion, our results indicate that predictability decreases early preparatory control demands (via left PRE) and increases preparatory temporal attention processes (via right ITG)

1.5. Dissemination

Conference presentation
Ignatiadis K., Boncz A., Baier D., Winkler I., Baumgartner R., Toth B: Temporal expectations modulate coupling between primary auditory and higher-level cognitive control regions In: SAMBA Salzburg Mind-Brain Annual Meeting 2021 (2021) Paper: poster

The manuscript is in preparation.

2. The effects of aging and hearing impairment on listening in a noisy environment

2.1. Background

Listening in noisy environments is a fundamental capability of the human hearing system. It is relying on functions such as integrating sound elements into a meaningful object while perceptually separating it from the rest of the acoustic environment. Aging may compromises either central processes (i.e. Figure-Ground Segregation ability; speech in noise performance) or peripheral processes (i.e. cochlear synaptopathy; degraded outer hair cells). The purpose of the current study was to test the causes of impaired listening in noise in aging. To separate the effects of age and age-related hearing loss, three groups of listeners (young adults; normal-hearing elderly, and hearing-impaired elderly) have been tested. The group of hearing-impaired elderly was selected based on an elevated pure-tone audiometric threshold, thus assuring deterioration of peripheral function (Slade et al 20205). The effects of differences in peripheral gain and cognitive load (e.g., effects of the inter-individual variation in working memory capacity) between the groups were reduced by keeping task performance approximately equal across all listeners using individualized stimuli. Because performance in psychoacoustic measures inevitably combines the effects of peripheral and central processes, ERP measures (specifically ORN and P400) were collected to shed light on the underlying processes.

2.2. Methods

Participants, procedure, and stimuli: Participants were selected based on pure tone audiometric thresholds (serves as a proxy of peripheral auditory function measure:): Three groups: Young (N=21, mean age=21.2 yrs), Elderly with normal hearing (N=13, mean age=67.3 yrs), Hearing impaired elderly (N=16, 68.7 yrs). Participants were presented with stimuli concatenating 40 chords of 50 ms duration (Figure 1A). Half of the stimuli included a figure (a set of tones rising together in time embedded in a cloud of randomly selected tones; Figure trials), while the other half consisted only of chords made up of randomly selected frequencies (No-Figure trials adapted from Toth et al 2016). Listeners performed the figure

detection task under low noise (LN) and high noise (HN) conditions, which differed only in the number of concurrent randomly varying (background) tones. Stimulus individualization was achieved through two adaptive threshold detection procedures conducted before the main figure detection task. First, low-noise stimuli were adjusted for each participant by manipulating the number of tones belonging to the Figure (figure coherence) so that participants performed figure detection at 85% accuracy. Second, high-noise stimuli were adjusted for each participant by increasing the number of background tones in the LN stimuli until the participant performed at 65% accuracy.

Behavioral data analysis: From the threshold detection tasks, we analyzed the participants' coherence level in the LN condition, the number of additional background tones in the HN condition, and log-transformed SNR values for both conditions. A mixed-model ANOVA with the within-subject factor NOISE (LN vs HN) and the between-subject factor GROUP (young adult, normal-hearing elderly, hearing-impaired elderly) was conducted on SNR. For coherence levels (LN only) and the number of additional background tones (HN only), one-way ANOVAs were performed with the between-subject factor GROUP (young, normal-hearing old, hearing-impaired old). From the main task, detection performance was assessed by the sensitivity index, false alarm rate (FA), and mean reaction times (RT). Mixed-mode ANOVAs were conducted with the within-subject factor NOISE, and the between-subject factor GROUP, separately on d', FA, and RT.

EEG data analysis: Epochs were extracted from the continuous EEG records between -800 and +2300 ms relative to the onset of the Figure in Figure trials. For No-figure trials, onsets were selected randomly from the set of Figure onsets in the Figure trials (each Figure onset value from Figure trials was selected only once for a No-figure trial). Artifact removal was performed with ICA and an automatic threshold detection (+/- 100 μV) procedure. EEG source localization using sLORETA was based on the combination of individual MRIs and adjusted default electrode positions. Brain activity within the time windows corresponding to the ORN and P400 ERP components was measured separately for each stimulus type/condition/group. Time windows were defined by visual inspection of grand average ERPs. The effects of age were tested with mixed mode ANOVAs with within-subject factors FIGURE (Figure vs No-figure), NOISE (LN vs. HN), LATERALITY (left vs midline vs right), and the between-subject factor AGE (young adult vs normal-hearing elderly) on the two ERP amplitudes and peak latencies. Similar mixed-mode ANOVAs were conducted to test the effects of hearing impairment by exchanging AGE for the between-subject factor HEARING IMPAIRMENT (normal-hearing vs hearing-impaired older adults). Post-hoc pairwise comparisons were computed by Tukey HSD tests.

2.3. Results

Behavioral results

Pretest calibration verified: From Figure and BG tone distribution across subjects we calculated the average SNR values for high and low noise stimulus. As was intended the SNR was significantly lower for high relative low noise conditions. Detection accuracy showed no differences across groups. Stimulus calibration successfully compensated for individual performance differences.

Hearing impairment has an effect on FGS ability The figure coherence values needed to reach the same performance in the high-SNR condition were significantly higher for the

hearing-impaired elderly than for the other two groups. Similarly, the hearing-impaired group needed a significantly higher ratio between figure coherence and noise to reach the same performance in the low-SNR condition than the other two groups. In conclusion hearing, impaired elderly have problems with grouping tones.

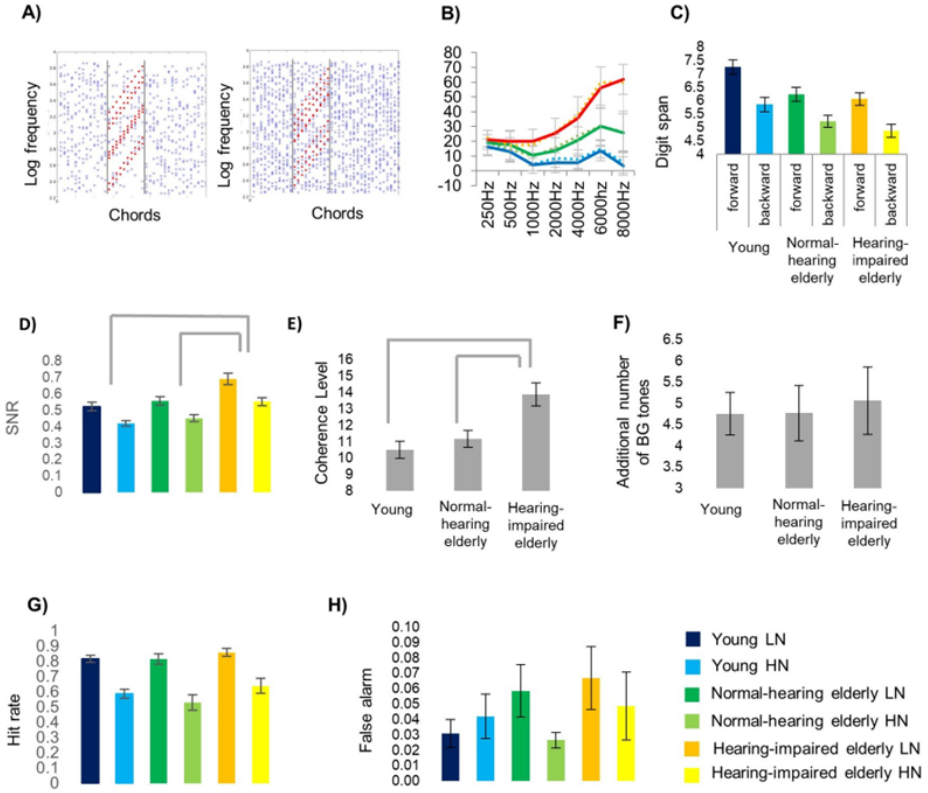

Figure 1. (A) Figure Examples of stimuli for the low (LN) and high noise (HN) conditions, respectively. (B) Mean pure tone audiometry thresholds for the young, adult (blue line; N=20), normal-hearing, elderly (green line; N=13), and hearing-impaired older listeners across elderly groups (red line; N=16) in the 250 - 8000 Hz range. Error bars depict SEM on all graphs. (C) Forward and backward digit span performance (corresponding to working memory capacity and control) for the three groups. (D) Mean SNR values were derived from the threshold detection tasks ((across LN and HN) from the stimulus individualization procedure. (E) Mean figure coherence level derived from the first threshold detection task (and employed later in the FG segregation task) for the three groups. Mean Figure coherence level of the LN stimuli for the three groups.; significant group differences ($p<0.01$) are marked by gray lines above the bar charts. (F) The mean increase in the background tone number between the tones from LN to HN conditions for the three groups. (G-H) Behavioral performance (Hit rate and false alarm rate, respectively) in, separately for LN and HN; color labels are at the FG segregation task lower left corner of the figure.

EEG results

The ORN amplitude showed an effect of SNR. The main effect of SNR was significant due to a higher ORN for high- than low-SNR trials. Figure events elicited ORN between 250 and 350 ms latency from Figure onset in the young adult group while between 350 and 550 ms in the normal-hearing and hearing-impaired elderly groups. There was a significant main effect of AGE, with the ORN peak latency delayed in normal-hearing elderly (M = 421 ms) compared to young adults (M = 280 ms). The three-way interaction of FIGURE × NOISE ×

HEARING IMPAIRMENT was significant. This effect was further analyzed with repeated measures ANOVAs including only Figure trials measured at the C3 electrode (due to the left central ORN distribution), separately for the normal-hearing and hearing-impaired elderly groups. In the normal-hearing elderly group, Figure stimuli elicited significantly larger ORN in the HN relative to LN condition, whereas no significant NOISE effect was found in the hearing-impaired elderly group. The brain regions activated during the ORN period were identified by source localization performed on the responses elicited by Figure trials. The sensitivity to signal-to-noise ratio was tested by comparing the source signals between the LN and HN conditions, separately for the young adult, normal-hearing, and hearing-impaired elderly groups by permutation-based t-tests. Significant NOISE effects were found predominantly in higher-level auditory and associational areas such as the left temporal cortices, the planum temporale (PT), and the intraparietal sulcus (IPS) Figure 2C). In young listeners, precentral cortical regions were also significantly sensitive to the signal-to-noise ratio.

Figure elicited P400 response while background no. The P400 amplitude showed an effect of age but no effect of SNR or hearing impairment. The P400 response showed higher amplitude in young subjects than in elderly subjects with or without hearing impairment. The two elderly groups did not significantly differ from each other. Generally, we found lower P400 amplitude in the elderly relative to the young

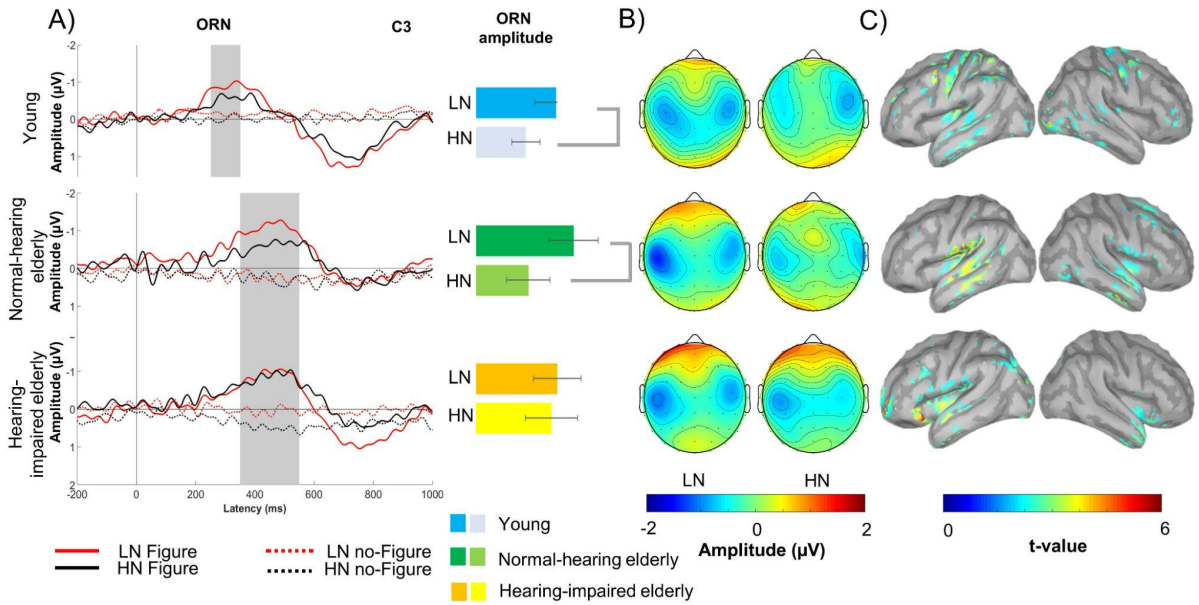

Figure 2. A) Group-averaged (young adult: N=20; normal-hearing elderly: N=13; hearing-impaired older elderly: N=16) central (C3; maximal ORN amplitude) ERP responses to Figure (solid line) and noNo-Figure (dashed line) related central (C3 lead) ORN elicited stimuli obtained in the LN (red) and the HN condition (black) respectively for young normal-hearing and hearing-impaired older listeners.). Zero latency is at the onset of the Figure event. Gray vertical bands show the measurement window for ORN while the yellow dashed line indicates the latency. The bar charts on the right side of ORN in young adults. On the panel shown on the right, the effect of NOISE is shown on the barplot for mean ORN amplitude respectively for amplitudes (with SEM) separately for the LN and HN conditions and groups. Significant NOISE effects ($p<0.05$) are marked by gray lines beside the bar charts. B) Scalp distribution of the ORN responses to Figure elicited ORN response respectively stimuli for the LN and HN conditions and groups with color scale below. C). Source localization results of) Brain areas sensitive to the NOISE effect (HN vs. LN condition) within the ORN time

window. C) Significant NOISE effect on source activity (current source density based on dSPM) found in young normal-hearing and hearing-impaired older adult groups separately. (color scale below).

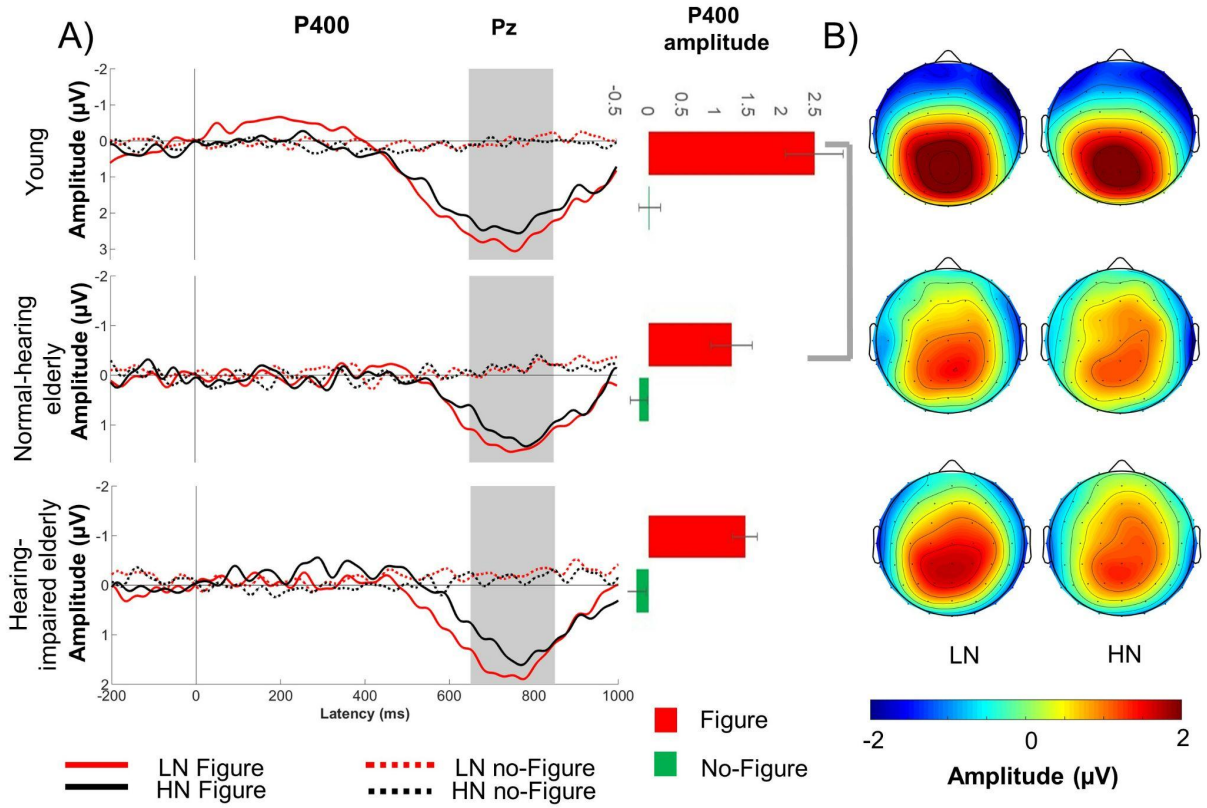

Figure 3. A) Group-averaged (young adult: N=20; normal-hearing elderly: N=13; hearing-impaired older elderly: N=16) parietal (Pz; maximal P400 amplitude) ERP responses to Figure (solid line) and No-Figure (dashed line) related parietal (Pz lead) p400 elicited stimuli obtained in the LN (red) and the HN condition (black) respectively for young normal-hearing and hearing-impaired older listeners.). Zero latency is at the onset of the Figure event. Gray vertical bands show the measurement window for P400. On the right, the effect of FIGURE is shown The bar charts on the barplot for the right side of the panel show the mean P400 amplitude respectively for Figure and no-Figure trial and groups. Amplitudes (with SEM) separately for the LN and HN conditions. Significant group effects ($p<0.05$) are marked by gray lines beside the bar charts. B) Scalp distribution of Figure elicited the P400 response respectively responses to Figure stimuli for the LN and HN conditions and groups with color scale below.

2.4. Discussion

We tested the contributions of peripheral and central auditory processes to age-related decline of hearing in noisy environments using a tone-cloud-based figure detection task. We found that while aging slows the processing of the concurrent cues of auditory objects (long ORN latencies in the elderly groups) and may affect processes involved in deciding the task-relevance of the stimuli (lower P400 amplitude in the normal-hearing elderly than the young adult group), overall, it does not significantly reduce the ability of auditory object detection in noise (no significant differences in the signal-to-noise ratios between the young

adults and the normal-hearing elderly group). However, when aging is accompanied by higher levels of hearing loss, grouping concurrent sound elements suffers and, perhaps not independently, the tolerance to noise decreases, as higher coherence was needed by the hearing-impaired than the normal-hearing elderly group for the same figure detection performance, hearing thresholds negatively correlated with the number of background tones reducing detection performance from the LN to the HN level, and the ORN amplitudes did not significantly differ between the HN and LN condition in the hearing-impaired elderly group (while they differed in the other two groups). The inference about the effects of peripheral hearing loss is strongly supported by the efficacy of the stimulus individualization procedure: there are no significant group differences and no significant correlation between hearing thresholds and performance measures of the figure detection task, and no correlation between the current working memory indices and any of the behavioral measures. Further, the current results are fully compatible with those of prior studies showing that spectrotemporal coherence supports auditory stream segregation (better figure detection performance with higher coherence Slade et al 2020; Bendixen et al., 2010; Andreou et al 2011; Neubert et al 2021).

This work provides new information about the contributions of central and peripheral causes to the typical age-related decline of listening in a noisy environment. Behavioral and neurophysiological data collected in a well-controlled model of listening in noise suggest that aging alone does not significantly reduce the ability to detect sound sources in a complex auditory scene. However, even mild hearing impairment significantly reduces this ability. The stimulus paradigm used appears to be quite sensitive to hearing loss, making it potentially useful for the early detection of hearing problems.

2.5. Dissemination

Tóth Brigitta: EARLY SIGNS FOR AGE-RELATED NEURAL DECLINE IN THE CENTRAL AUDITORY PATHWAY DURING LISTENING IN A NOISY ENVIRONMENT, In: Salzburg Mind Brain Annual Meeting (SAMBA) 2022, (2022) p. 64., 2022

Tóth Brigitta, Ádám Boncz, Szalárdy Orsolya, Péter Velősy, István Winkler: Auditory figure-ground segregation is impaired by aging and age-related hearing loss, In: 20th World Congress of Psychophysiology (IOP2021), (2021) meghívott előadás, 2021

Péter Kristóf Velősy, Ádám Boncz, István Winkler, Brigitta Tóth: Auditory Figure-Ground Segregation is impaired by aging and age-related hearing loss, In: SAMBA Salzburg Mind-Brain Annual Meeting 2021, (2021) poster, 2021

Péter Kristóf Velősy, Ádám Boncz, István Winkler, Brigitta Tóth: Auditory Figure-Ground Segregation is impaired by aging and age-related hearing loss, In: 5th international conference of the European Society for Cognitive and Affective Neuroscience, ESCAN 2021, (2021) A-0545, 2021 *

Péter Kristóf Velősy, Ádám Boncz, István Winkler, Brigitta Tóth: Auditory Figure-Ground Segregation is impaired by aging and age-related hearing loss, In: 12th Dubrovnik Conference on Cognitive Science Linguistic & Cognitive Foundations of Meaning, (2021) poster, 2021 *

The manuscript is published at.
Ádám Boncz, Orsolya Szalárdy, Péter Kristóf Velősy, Luca Béres, István Winkler, Brigitta Tóth The effects of aging and hearing impairment on listening in noise bioRxiv 2023.01.20.524873; doi: https://doi.org/10.1101/2023.01.20.524873

3. Neural bases of auditory statistical learning by automatic tracking of sensory sequence structure in newborns

3.1. Background

The seemingly effortless ability of our auditory system to rapidly detect new events in a dynamic environment is crucial for survival, especially for a newborn organism. Whether underlying brain processes are innate is unknown. In the present study electroencephalography was recorded while regularly patterned (REG) versus random (RAND) tone sequences were presented to newborn infants during they were asleep. Regular relative to random sequences elicited differential neural responses indicating an innate capacity of the auditory system to form object representations as early as following the second repetition of a tone pattern. We demonstrate that newborns perform on par with an ideal observer model (the probabilistic predictions of a variable-order Markov model). This evidence indicates that the auditory system is capable of forming and automatically and continuously maintaining the representation of ongoing sensory input. The statistically regular arrangement of the sensory input enhances the system to detect changes in the auditory input and update its representation accordingly. Evidence on how the newborn's brain tracks the statistics of past sensory input has not been tested. In the present study, we aim to observe neural correlates when in which brain areas support discovering the regularity within the ongoing sound sequence in the newborn's auditory system. We recorded the EEG in newborn infants exposed to tone sequences that were unique on each trial (implemented from the study of Southwell and Chait (2018) thereby each trial required a buildup of a novel regularity representation. One standard tone sequence consisted of regular (REG) the other only random (RAND) tones otherwise matched frequencies (see Fig. 1). In other words the frequency of the successive tones was highly predictable in the regular while unpredictable for the RAND sequences. Based on the hypothesis that the adult brain monitors incoming sensory information against the specific internal model established by the prior statistics of the sensory input, we expect regular tones (REG) to elicit stronger neural activity than RAND sequences. Our study investigates this question in newborns by measuring neural response to REG and RAND sequences.

3.2. Methods

Participants, procedure, and stimuli: The participants of the study were 33 healthy, full-term newborns (0–4 days of age, 17 male, 16 female, mean gestational age of 43.24 weeks, SD = 2.39). The stimuli used in this experiment, illustrated in Figure 1, were based on the study of Southwell & Chait (2018). 3000 ms long tone sequences were created from 50 ms long pure tones of a 198–3563 Hz frequency range. The tones were organized in a regular (REG) or random (RAND) frequency arrangement. Each sequence contained 10 unique frequency components. In REG sequences, these frequencies were arranged in a 10-tone pattern, which was then repeated 6 times (60 tones of 50 ms each amounting to the 3000 ms stimuli).

Corresponding RAND stimuli were generated for each REG sequence by randomizing it, with the caveat that two tones of the same frequency cannot follow each other directly. To ensure that each stimulus contains roughly the same bandwidth of frequency components, the tones were picked from a set of 26 tones of 198–3563 Hz (logarithmic spacing, 12% increase per step), first choosing a random subset of 13 adjacent tones, then using 10 of these tones at random to create a stimulus. The newborns were asleep during the duration of the stimulus presentation. 960 stimuli – 240 of each of the 4 conditions were presented in pseudorandom order with an inter-stimulus interval (ISI) of 900 to 1300 ms chosen randomly.

EEG data analysis: Recordings were epoched separately for the REG-RAND response analysis. Epochs were extracted between -500 and +3500 ms relative to the onset of the sequence respectively for both REG and both RAND conditions. Baseline correction was based on a 100 ms prestimulus interval. Artifacts were removed based on visual inspection. The epoch count was equalized across conditions for each subject. For comparing the overall difference between REG and RAND trials, the global field power (GFP) was estimated as the root mean square of the signal at all electrodes for each time point to give a time series that reflects the instantaneous power of the evoked response (based on Southwell and Chait, 2018). The statistical comparison of GFP between all REG and RAND was assessed using cluster-based permutation statistics at each time sample, from sequence onset to 3000 msec following offset. t-tests (2-tail) were performed using t-statistics computed on clusters in time and controlled for a family-wise error rate of 0.05 using 10000 permutations to create the null model (Maris & Oostenveld, 2007).

EEG source localization: The age-appropriate brain template (for 0.5 months provided by O'Reilly) was segmented based on the default setting and was entered, along with default electrode locations, into the forward boundary element head model (BEM) For the modeling of time-varying source signals (current density) of all cortical voxels, a minimum norm estimate inverse solution was applied using dynamical SPM normalization. Finally, the average signal for the corresponding time window of interest (1.048–1.594 s, for RAND and REG stimulus types, was entered into a permutation-based (N=1000) paired sample t-test (alpha level=0.01).

Ideal observer Model of the REG and RAND tone sequences. A variable-order Markov model was used to quantify the predictability of each tone-pip within the presented tone sequences (64 65, 66). Here, we use the responses of the model as an ideal observer to compare with those of the participants. Information Dynamics of Music (IDyOM) uses unsupervised statistical learning to acquire transitional dependencies through exposure to sequences of auditory events. The model's output at each tone-pip position within a sequence is a conditional (or posterior) probability distribution governing the frequency of the next tone-pip, given the preceding context. This distribution accumulates the model's experience during the experimental session. Using the posterior distribution, the model estimates the predictability of each possible continuation tone, including the tone that actually follows. The model's output is formalized using the information-theoretic concept of information content (IC). IC is the negative log probability (–log P) of a tone and is used as a measure of the unexpectedness of each tone in the sequence, given the preceding context. The model is predominantly used to provide a benchmark for the earliest time at which RAND-REG (and REG-RAND) transitions can be detected. This time point is quantified by identifying the

tone-pip position for which the IC begins to deviate (fall or rise). The computed IC time series for RAND or REG with a cluster-based permutation test.

3.3. Results

The global field potential (GFP) was significantly larger in RAND than in REG trials (Figure 1). Temporal clusters with a significant difference between RAND and REG were identified at 1048–1594 ms ($p=0.045$) and at 2580–3500 ms ($p=0.022$) after stimulus onset. This means that deviation commenced after two cycles of a pattern were completed in the REG condition. Source localization revealed that REG vs RAND effect on sequence evoked responses is generated exclusively on the right hemisphere. Specifically, the generators were observed in the parietal cortex (Inferior parietal (IPG) and supramarginal (SMG) postcentral gyrus).

The Ideal observer IDyOM computational model was computed for the REG and RAND tone sequences, then compared with a cluster-based permutation test. The significant cluster, where the information content of random and regular stimuli diverge, is located between tones 11 to 60 ($p<0.001$), i.e. it falls within the second repetition of the sequence in regular trials.

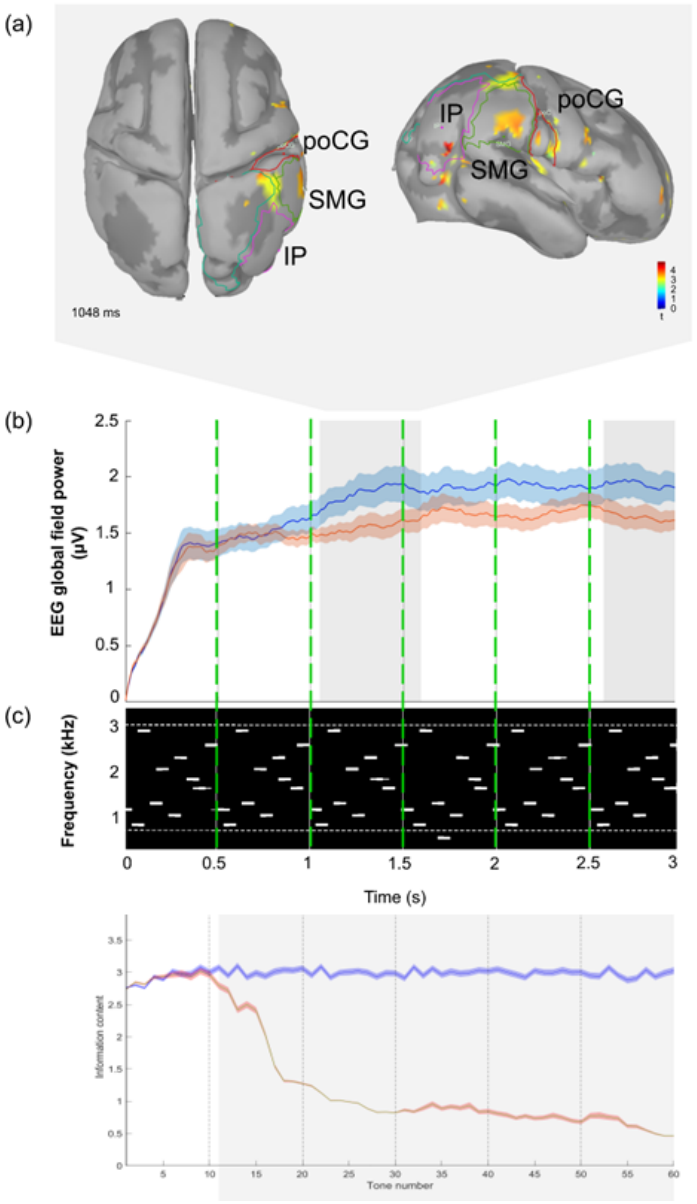

Fig 1. a) Significant REG-induced EEG source activity with top and left view **b)** GFP responses for REG and RAND stimuli. Gray-shaded areas represent significant differences **c)** the semantic figure of the REG stimuli. **d)** Time series resulted from the Ideal observer IDyOM computational model computed for the REG and RAND tone sequences. Information Content (IC) predicted by the IDyOM model when trained on random and regular stimuli from our experiment. The shaded area indicates a significant cluster resulting from cluster-based permutation testing.

3.4. Discussion

The present study is aimed to address 1) the innate nature of predictability influences of rapid tone sequences on neural responses. We replicated previous results by Southwell et al., 2017 and Southwell and Chait 2018 and demonstrated the effects of context (REG vs RAND) on the brain response to the sequence. Although for adults the observed effect was a

higher response for regular than random sequence while for newborns it was the opposite. It is likely that due to the lack of maturation such as myelination the polarity of event-related neural responses changes. Concordantly to studies on adults (Southwell and Chait 2018), we further observed the effects of sequence context on the response to the deviant. Specifically, the frequency deviants exclusively within regular sequences evoked a larger response (from 50 msec after outlier onset) and then matched deviants in random sequences. Below we further discuss how the newborn auditory system automatically tracks and represents the unfolding structure in dynamic sensory signals. Robust effects of predictability (regular context) were observed despite the fact that patterns were never repeated and had to be discovered anew on each trial. In conclusion, the present results indicate that implicit models based on regular statistical patterns of the acoustic input are an innate property of the auditory system that strongly relies on the left primary auditory and secondary association cortices. There is a slight time lag between the neural responses for regularity in the newborn nervous system relative to what was expected from the ideal observer model. This indicates that the auditory system is still immature, and by time via plasticity, it is going to develop to reach the performance of an ideal observer.

3.5. Dissemination

Conference presentation:
Peter Velősy, Brigitta Tóth, Gábor P. Háden, István Winkler: Newborn infants differently process random and regular tone sequences, In: Salzburg Mind-Brain Annual Meeting (SAMBA) 2022, (2022) p. p60., 2022 *

The manuscript is in preparation.

4. Early maturation of sound duration processing in the infant's brain

4.1. Background

The ability to process sound duration is crucial already at a very early age for laying the foundation for the main functions of auditory perception, such as object perception and music and language acquisition. With the availability of age-appropriate structural anatomical templates, we can reconstruct EEG source activity with much-improved reliability. The current study capitalized on this possibility by reconstructing the sources of event-related potential (ERP) waveforms sensitive to sound duration in four- and nine-month-old infants. We investigated duration-sensitive auditory ERP waveforms and their sources to establish their developmental changes between four and nine months of age. To our knowledge, this is the first study applying age-appropriate templates published by O'Reilly and colleagues (2020) [25] to reconstruct the sources of auditory ERPs in infants.

Infants were presented with four sounds differing in duration (200 vs. 300 ms) and sound quality (harmonic tones vs. white noise). We expected to find significant changes in ERP morphology between the two age groups in accordance with previous descriptions of ERP development. Indeed, in contrast to the simpler ERP component structure at four months, by nine months of age, we expected to find precursors of the adult ERP complex in the form of a positive deflection, accompanied by two negative ones coinciding with the N250 and the N450 latencies (Pearce, 2005). We then asked whether either or both

waveforms show sensitivity to sound duration and whether sensitivity to sound duration is dependent on the quality of the sound (harmonic tones vs. noise segments).

4.2. Methods

Participants, procedure, and stimuli: Infants were recruited as part of a broader longitudinal study the first one comprised 64 (20 males) four-months-old, and the second cohort was 63 (19 males) nine-months-old healthy full-term infants. Due to the longitudinal nature of the study, 9 of the infants in the final sample were tested at both four and nine months.

All infants were presented with shorter (200 ms) or longer (300 ms) sounds grouped into two separate blocks each consisting of 150 short and 150 long sounds delivered in random order. One of the stimulus blocks presented tones of 500 Hz base frequency with 3 harmonics of 50, 33, and 25 percent amplitude, respectively, summed linearly together ('tone' condition). The other stimulus block comprised frozen white noise segments ('noise' condition). All sounds were presented at approximately 70 dB SPL loudness and the sounds were attenuated by 5 ms long raised-cosine onset and offset ramps. The onset-to-onset interval was 800 ms. The tone condition was always delivered first, and there was a short rest of 30-60 seconds between conditions.

The infant sat comfortably in her mother's lap while the experimenter employed toys to keep the infant facing toward the loudspeakers and her attention away from the electrode net. The mother was listening to music through closed-can audiometric headphones to isolate her from the experimental stimulation. If the infant became fussy, the playback was stopped, and the experimenter attempted to pacify her. If pacifying was successful the playback restarted from the beginning, otherwise, the experiment was discontinued.

EEG data analysis: Artefacts were eliminated from the 64-channel EEG data with ICA analysis on the 45 PCA-reduced components after re-referencing them to the average reference. The topographical distribution and frequency contents of the ICA components were visually inspected, and the components constituting oculomotor, cardiac, muscular, or line artifacts were manually removed. From the continuous EEG records, epochs were extracted between -100 and 800 ms relative to the sound onset, separately for the two STIMULUS DURATIONs (short- and long-duration sounds), STIMULUS TYPEs (tones and noises), and AGE GROUPs (four- and nine-month-olds). The average voltage in the -100 and 0 ms windows served as the baseline. A threshold of +/- 150 μV was set to reject epochs with abrupt amplitude changes, while thresholds of 100 μV over the whole epoch for slope and 0.5 r2 were set to remove epochs with step-like artifacts and linear trends. Infants' data was not used if the remaining number of epochs for each STIMULUS DURATION was under 75 for either STIMULUS TYPE.

EEG source localization: For the modeling of time-varying source signals (current density) of all cortical voxels, a minimum norm estimate inverse solution was applied after appropriate noise covariance estimation. Finally, for all ROIs, we extracted the average signal for the corresponding ERP peak windows, separately for each SOUND DURATION (short, long), STIMULUS TYPE (tones, noise), and AGE GROUP (4, 9 months). For statistical analyses, average source amplitudes in the selected regions were tested separately for the early and late time windows, for tones and noise segments, and ROIs by between-subjects ANOVAs with the AGE GROUP factor (four-, nine-months-olds). All other aspects of the statistical analysis are identical to that employed for ERPs.

4.3. Results

Two successive front-centrally negative sound-duration sensitive waveforms were identified in the ERPs elicited by nine-months old infants. In contrast, only the first of these two negativities were present in the responses of four-month-olds with similar, 350-400 ms peak latencies in the two age groups. The late negativity peaked between 580 and 650 ms in the nine-month-olds over fronto-central scalp sites. The emergence of a second sound duration-sensitive waveform between four and nine months of age may reflect that this information is further processed in the latter age group.

Two temporally separate ERP waveforms were found to be modulated by sound duration. Generators of these waveforms were mainly located in the primary and secondary auditory areas and other language-related regions, such as the superior temporal and the inferior frontal gyri. The results show marked developmental changes between four and nine months, partly reflected by scalp-recorded ERPs, but appearing in the underlying generators in a far more nuanced way. The results also confirm the feasibility of the application of anatomical templates in developmental populations.

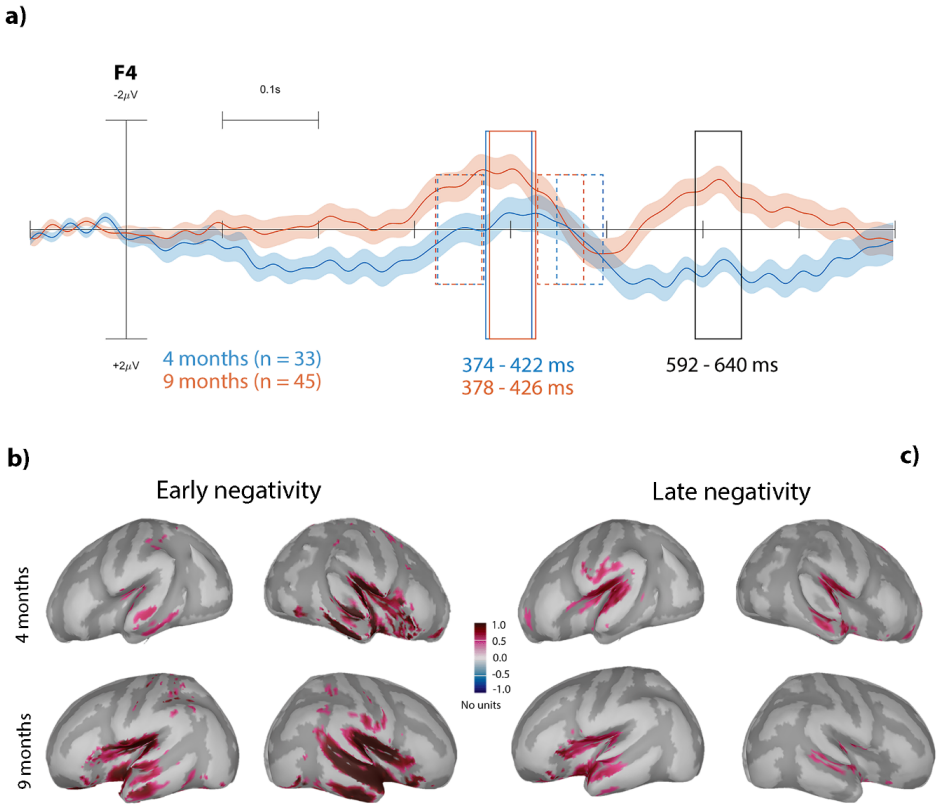

Figure 1: Grand average ERP difference waveforms elicited by tones. Panel **A)** plots the right frontal (F4) ERP responses of the two age groups (marked by line colors). The early and late measurement windows are shown with rectangles drawn with solid lines (the exact range shown under the rectangle). The rectangles with dashed lines refer to the reference interval used for calculating the amplitudes for the early waveform. Panels **B)** and **C)** show the distribution of the average current source density (CSD) over the inflated cortex during the early (panel **B**) and late (panel **C**) duration-sensitive ERPs elicited by tones. The upper row

presents the four-month-old infants' data, the lower that of the nine-month-olds. The color scale is at the center of the cortical distribution panels.

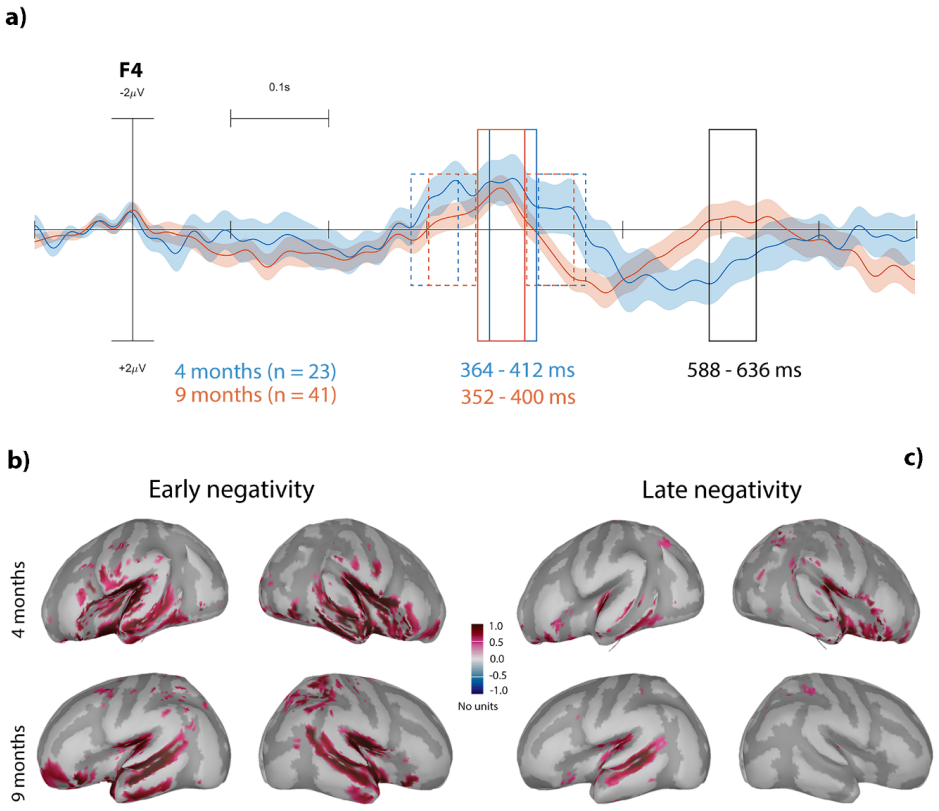

Figure 2: Grand average ERP difference waveforms elicited by noise segments. Panel **A)** plots the right frontal (F4) ERP responses of the two age groups (marked by line colors). The early and late measurement windows are shown with rectangles drawn with solid lines (the exact range shown under the rectangle). The rectangles with dashed lines refer to the reference interval used for calculating the amplitudes for the early waveform. Panels **B)** and **C)** show the distribution of the average current source density (CSD) over the inflated cortex during the early (panel **B**) and late (panel **C**) duration-sensitive ERPs elicited by noise. The upper row presents the four-month-old infants' data, the lower that of the nine-month-olds. The color scale is at the center of the cortical distribution panels.

4.4. Discussion

Results of the current study showed that the brain of four- and nine-month-old infants is sensitive to sound duration, as reflected by ERPs elicited by short, isolated sounds. Effects of maturation were found for the scalp-recorded waveforms and the corresponding source activity. Both scalp-recorded ERPs and the related source activity became stronger and spatially better defined between four and nine months of age. Generators of the event-related potentials sensitive to sound duration were located in the ventral frontotemporal auditory pathway. Details of the results are discussed below.

The ERP results are generally congruent with reports of waveforms related to the N250 and N450 in infant studies with duration manipulation (Pearce 2005; Pearce et al.,

2010; Pearce, & Wiggins, 2006; Kushnerenko et al 2001). The fronto-centrally maximal scalp distributions of the current waveforms are also compatible with those reported in previous literature (Pearce, & Wiggins, 2006; Kushnerenko et al 2001, 2002). This fronto-central gradient has been suggested to be part of the developmental trajectory of auditory ERPs (Kushnerenko et al 2002).

The source-localized results show that the generators underlying the early negativity are distributed exclusively within the ventral auditory pathway consisting of bilateral temporal (PAC, MTG, STG, ITG) and inferior frontal cortices. The neural generators of the late negativity were located in overlapping areas. However, they showed more focal distribution within primary and secondary auditory areas. The duration-sensitive sources found in this study are consistent with those reported in the literature in response to both speech sounds and tones: the superior temporal, supramarginal, and inferior frontal gyri, and primary and secondary auditory cortical areas (Adibpour, et al., 2008; Van den Heuvel 2015; Hämäläinen et al., 2008). This points towards the reliability of the use of anatomical templates in developmental samples, which represents an important turning point in studying electrical brain activity in infants.

The similarity between the results in the two age groups sheds light on the central role the processing of temporal information plays in sound processing: the processing of temporal features is more consistent than that of spectral features throughout development and even its neural substrates may not change dramatically from infancy to adulthood. Thus, whereas pitch discrimination initially requires a very large separation between the sounds to elicit reliable discriminative brain activity (Li, et al., 2019), temporal features are reliably detected already at birth (Novitski et al 2007; Kushnerenko et al 200) and responses sensitive to different sound durations are quite similar between neonates and adults (Kushnerenko et al 2001). The cortical distribution of the neural activity within the late negativity time window also strongly overlapped between age groups. However, substantial age-related differences were found in the left primary and secondary auditory areas (bilateral STG, bilateral PAC, left bank of the STS, left ITG, and left MTG). These distributions indicate that maturation aids auditory network development in a quantitative manner at the later stages of duration processing. Age-related effects on duration-sensitive ERPs and their generators may stem from multiple types of maturational processes (Kushnerenko et al 2001, 2002). For example, myelination of auditory pathways plays a crucial role by enabling rapid coordination among neurons (Ruhnau et al., 2011). These findings suggest that the frontal cortices and their connections to auditory sensory regions (temporo-parietal areas) play a major role in language acquisition.

The current results provide new information on the development of the processing of an important temporal parameter, sound duration. The ERP results are generally compatible with those from previous studies. The more reliable source reconstruction offered by the recently released infant structural anatomical templates provided new insights into the generators underlying duration processing and their development, allowing one to speculate about the functional and developmental significance of this neural activity. Naturally, these initial hypotheses require further studies for confirmation and specification.

4.5. Dissemination

Manuscript published at:
Polver, S.,, Háden, G.P., Bulf, H., & Toth, B. (2023, preprint). Early maturation of

sound duration processing in the infant's brain. bioRxiv. doi: 10.1101/2023.01.24.525349

5. Spatial cues can support auditory figure-ground segregation

5.1. Background

Spatial information is utilized in the processing of complex auditory scenes [for review see Bizley and Cohen (2013); Shinn-Cunningham et al. (2017)]. For stimuli consisting of brief tone bursts with randomly selected frequencies, the detection of a target tone frequency that is repeated in successive bursts can be improved using spatial cues (Kidd et al., 1994). Specifically, when the repeated target tone bursts are presented to one ear, detection of the target is improved when the interfering tones are presented to both ears instead of being presented only to the ear in which the target tones are presented. These results show that perceived differences in location promote the perceptual segregation of the target and masker. Spatial information can also aid in detecting patterns of tones when they are presented amid other randomly varying task-irrelevant tones

The present study aims to investigate more systematically whether spatially separating a complex auditory "figure" from the background auditory stream may enhance the detection of a target in a cluttered auditory scene.

5.2. Methods

Participants, procedure, and stimuli: Ten individuals (seven male, three female) participated in the current study with age ranging from 18 to 34 yr (mean 25.2). Throughout the study, participants were instructed to indicate whether or not they detected the presence of a figure by pressing one of two response buttons at the end of each trial. Each trial consisted of a sequence of 40 randomly generated chords of 50 ms duration. Chords were temporally adjacent and included 10 ms raised-cosine onset/offset ramps to reduce spectral splatter (spread of spectral content at abrupt onsets and offsets).All chords here contained a fixed number of ten tones. In half of the stimuli, four of the ten tones in a chord were repeated over either three or five chords. These repeated tones collectively formed a "figure" amid the background of random chords. The onset of these figure chords randomly occurred between the 15th and 20th chord (750–1000 ms after the stimulus onset) In the diotic condition (whether the trial included a figure or was a control trial), all tones were presented diotically, with at an ITD of 0 ls (target and background were both perceived at the midline). In lateral-burst figure trials, the figure tones were presented with an ITD of either þ685 ls or 685 ls (roughly at 690 perceived angle), whereas all background tones were presented diotically. In the lateral-burst control trials, a subset of the background tones (equal in number, duration, and temporal probability to the figure tones) was presented with an ITD of either þ685 ls or 685 ls while all other tones were presented diotically. In other words, in these trials, the whole background was presented at the midline at the start of the trial, while a portion of the background switched to a lateral position partway through the trial. In the lateral-stream conditions, for the entire duration of the trial, six of the ten tones in each background chord were presented diotically for the entire duration of the trial, while the remaining four tones

were presented at an ITD of either þ685 ls or 685 ls (lateral-stream control trials). In the lateral-stream figure trials, partway through the trial, the figure tones were added with an ITD that matched the ITD of the lateralized part of the ongoing background. The study included the lateral-stream condition as well, which was tested by an alternative explanation for the interference of lateralization observed in the Toth et al. (2016) study.

A series of five stimulus blocks with trial-by-trial feedback were delivered to participants during training. Following the training the experiemntal block were presented to the listeners. The grand total of 576 trials (48 trials for each of the 12 conditions) were broken into 16 blocks of 36 trials each. Block delivery was self-paced: Between blocks, participants could take a break. Within a block, we randomly intermixed different interaural conditions (diotic, lateral burst, and lateral stream) that had the same target duration (either 3 or 5). All participants were first presented with the (easier) five-chord duration trials (the first eight blocks). Because the focus of this study was to investigate differences related to the interaural conditions, this potential ordering effect of the duration parameter does not confound our intended research question while allowing for a shorter training session. Listeners were provided both trial-by-trial visual feedback (green cues after correct responses and red cues following incorrect responses) and a performance summary after each block.

Behavioral data analysis: The accuracy of discriminating figure and background-only trials was quantified using d0 (Green and Swets, 1966). A two-way repeated measures analysis of variance (ANOVA) was performed on the collapsed dataset with figure duration and interaural condition as within-subjects factors.

5.3. Results

Listeners were much better at detecting figures with longer duration, confirmed by the statistically significant main effect of duration. A main effect of interaural configuration was also observed. The interaction between figure/chord duration and interaural condition was not statistically significant. To assess differences in performance between the three interaural conditions for the two figure duration, a post hoc analysis was conducted. Results from paired t-tests indicate that listeners were better at detecting the figure in the lateral-burst condition as compared to the diotic condition for both figure durations three and five. Participants were also better at detecting the figure in the lateral-stream condition as compared to the diotic condition for figure duration five. With respect to the two binaural
conditions, detection performance was better in the lateral burst than in the lateral-stream conditions for figure duration three.

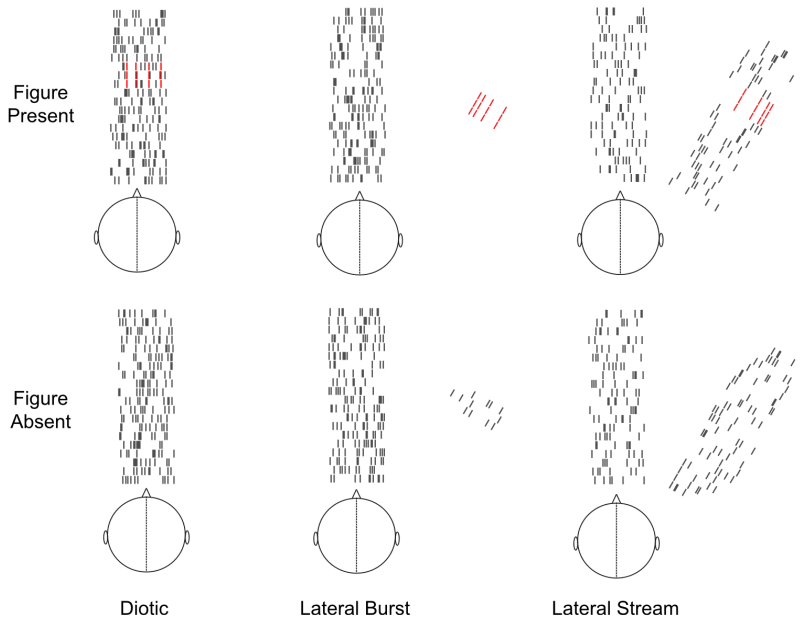

FIG. 1. (Color online) Schematic illustration of the figure and control (figure absent) trials for each of the three interaural conditions. The trial types are shown in separate rows and interaural conditions are shown in separate columns. Black vertical lines depict random tones (background) while red dotted lines represent repeating target patterns (figure). The perceived position of the stimulus is shown relative to the listener's head. In the diotic target and background were both perceived at the midline. In lateral-burst figure trials, the background was perceived at the midline (figure partway through the trial) and appeared at an angle to the left or to the right. In the lateral-burst control trials, at the start of the trial, the whole background was presented at the midline, while a portion of the background switched to a lateral position partway through the trial.

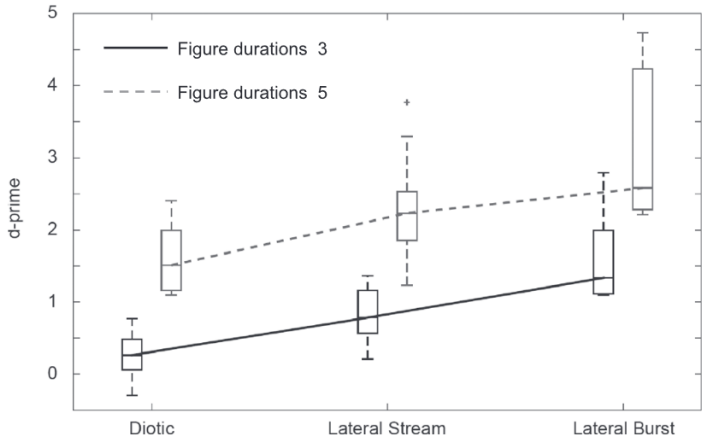

FIG. 2. Group-averaged (N ¼ 10) d0 values (standard error of mean represented by bars) are shown across the three interaural conditions and two different figure durations. The figure chord durations are marked by the white color for duration 3 and the dark grey color for duration 5. The three interaural conditions are shown in the three separate columns.

5.4. Discussion

Results of the presented experiment suggest that the previous negative results arose because of the specific experimental conditions tested. Here the authors find that ITDs provide a clear benefit for detecting a target tone sequence amid a mixture of other simultaneous tone bursts. Results demonstrate a clear benefit of spatial information on figure detection ability. Although this result is consistent with expectations derived from prior studies using similar stimuli (Kidd et al., 1994; Kidd et al., 1998), it conflicts with the findings of Toth et al. (2016). We argue that this discrepancy is most likely driven by differences in details of the experimental procedures and methods, ultimately concluding that binaural cues do indeed facilitate figure detection. The present study indicates that In the diotic and lateral-burst conditions, listeners must monitor a random background for the emergence of a repeated target that occurs at some unknown time; this regularity is more prominent when listeners need to monitor only a subset of background tones (lateral-burst configuration) than when they must monitor a denser background (diotic configuration). In contrast, in the lateral-burst condition, attention is drawn exogenously in both time and location to a small set of tones that are either repeated (target present) or unstructured (control), removing all temporal uncertainty. Thus, the current results suggest that the brief lateral event draws attention exogenously both to the direction and to the time at which the target will appear if it is present. This exogenous draw of attention appears to make it easier for the listener to decide whether that event is a repeated figure or a random pattern of background tones.

5.5. Dissemination

Reed, D. K., Chait, M., Tóth, B., Winkler, I., & Shinn-Cunningham, B. (2020). Spatial cues can support auditory figure-ground segregation. *The Journal of the Acoustical Society of America*, *147*(6), 3814. https://doi.org/10.1121/10.0001387

6. Supervised learning of listening in noise scenes is affected by age

6.1. Background

Listening in noisy environments is a fundamental skill for survival and social interaction. This skill depends on the ability to integrate sounds into a meaningful object while perceptually separating it from the rest of the acoustic environment (termed Figure–Ground Segregation - FGS). In older adults, the ability to separate target sounds from competing sound sources becomes compromised, leading to difficulties in understanding and conversing with others, with consequences for social integration and mental well-being (Snyder and Alain, 2007, Alain, Dyson, Snyder 2006). FGS is a constructive process that relies on the interaction between the incoming sensory information and prior knowledge about objects in the world (Bregman 1990, Winkler, et al., 2009). In most naturally cluttered scenes the sensory information that the ear receives is partial, distorted, or ambiguous therefore learning plays a crucial role in the recognition of perceptual objects (Shinn-Cunningham, 2008; Bizley & Cohen, 2013). The present study aims to understand major mechanisms for learning to segregate objects from complex scenes, and measure developmental changes in underlying neural plasticity for these mechanisms across the human lifespan (young to older adulthood).

The major mechanisms of learning - supervised reinforcement - will be investigated. Supervised learning refers to the ability to encode auditory events by detecting selectively attended targets in the environment (Jääskeläinen et al., 2011; Zhang & Kourtzi 2010, Gibson 1963).

4.2. Methods

Participants, procedure, and stimuli: In the present study supervised learning of FGS will be investigated in a training study with young and older adults. Data has been collected from twenty-one young adults (the planned N = 30 per group; age range 18-40 for young and 60-80 for elderly) Listeners will be trained on a perceptual discrimination task and their improvement will be measured over time. All the stimuli included a figure (a set of tones rising together in time embedded in a cloud of randomly selected tones; Figure trials).

These acoustic FG stimuli, implemented in my previous work (Tóth et al, 2016, developed by Teki et al., 2011; O'Sullivan et al., 2015, Shamma et al, 2011) aim to model the structure of natural complex acoustic scenes. The local spectral changes to the figure tones have a predictable influence on the perception of global forms (rising vs. falling figure patterns). In the discrimination task, listeners will report whether the figure was rising or falling.

Stimulus individualization was achieved through two adaptive threshold detection procedures conducted before the main figure discrimination task. The listener's task was to decide whether the Figure was rising all falling. First, low-noise stimuli were adjusted for each participant by manipulating the slope of tone frequencies of the figure (figure step size) so that participants performed figure detection at 80% accuracy. Following the discrimination, the task started with an individual setting but equalized difficulty. During the figure discrimination a staircase procedure was implemented by which the 3-down/1-up staircase method observer makes three consecutive correct responses, the stimulus level (e.g., slope) is reduced by the step size (multiplied by 1 − step size) in the next trial (3 down). If the observer makes a single incorrect response, the stimulus level is increased by the step size (multiplied by 1 + step size) in the next trial (1 up). A reversal (or endpoint) happens if the staircase changes its direction (from upward to downward or vice versa). We measure figure discrimination thresholds by averaging the stepsize at the last two-thirds of reversals in each staircase. In the 3-down/1-up staircase procedure, the estimated threshold in each measurement block is calculated by averaging stimulus levels at an even number of reversals after deleting the first four or five of them. We computed the block thresholds from the minimum step size in every block of trials.
The procedure included a pretest without feedback and two sessions (1 hour each) of the training with including feedback after each trial and finally with a posttest without feedback again.

Behavioral data analysis: These local properties of the figure stimulus and the background noise level (signal-to-noise ratio-SNR) will be separately and parametrically manipulated, allowing the experimenter to distinguish between two stages of FGS: 1) extraction of figure elements from a noisy background and 2) global discrimination between patterns of figures. We will test whether training improves both stages of FGS learning by applying a two-process mathematical model to fit figure discrimination thresholds across different SNRs, using methods pioneered by Kourtzi (Kuai & Kourtzi, 2013).

EEG data analysis: High-density EEG) recordings will be used to measure functional connections of the auditory cortices in relation to statistical or supervised learning (termed here as neural plasticity, Fell & Axmacher, 2011). Cortical sources will be re-constructed from high-density EEG activity, and phase synchronization of neural rhythms between sources will be assessed as a measure of the strength of functional connectivity (Stam et al., 2007).

EEG source localization: EEG source localization using sLORETA was based on the combination of template MRIs and adjusted default electrode positions. Brain activity within the time windows corresponding to the ORN and P400 ERP components will be source localized separately for each pre vs post-training/stimulus type/condition/group.

4.3. Results

Behavioral results Results of the preliminary analysis with 17 subjects. The mean minimum step size per session is shown below, calculated using two metrics the minimum step size reached in every staircase (block).

5.4. Discussion

As we expected training enhanced performance. We predict that it is going to hold for both younger and older adults, but to a different extent in each group. We predict that global pattern discrimination will be preserved in older age, whereas - due to reduced tolerance to background noise - figure extraction will be impaired in the elderly, mediated by weaker coupling between frontal and sensory cortices. This result would indicate that older adults may be able to compensate for hearing loss in noisy environments using global pattern discrimination abilities, but only if prior knowledge of sound source properties exists.

5.5. Dissemination

Data collection is finalized the data analysis and manuscript preparation is currently going on. Data will be published in a peer-reviewed journal.

Reference

Adibpour, P., Lebenberg, J., Kabdebon, C., Dehaene-Lambertz, G., & Dubois, J. (2020). Anatomo-functional correlates of auditory development in infancy. Developmental cognitive neuroscience, 42, 100752.

Alain, C., Dyson, B. J., & Snyder, J. S. (2006). Aging and the perceptual organization of sounds: A change of scene. Handbook of models for human aging, 759-769.

Aman, L., Picken, S., Andreou, L. V., & Chait, M. (2021). Sensitivity to temporal structure facilitates perceptual analysis of complex auditory scenes. Hearing Research, 400, 108111.

Anderson, B., & Sheinberg, D. L. (2008). Effects of temporal context and temporal expectancy on neural activity in inferior temporal cortex. Neuropsychologia, 46(4), 947-957.

Andreou, L. V., Kashino, M., & Chait, M. (2011). The role of temporal regularity in auditory segregation. Hearing research, 280(1-2), 228-235.

Arnal, L. H., & Giraud, A. L. (2012). Cortical oscillations and sensory predictions. Trends in cognitive sciences, 16(7), 390-398.

Auksztulewicz, R., Friston, K. J., & Nobre, A. C. (2017). Task relevance modulates the behavioural and neural effects of sensory predictions. PLoS biology, 15(12), e2003143.

Bendixen, A., Jones, S. J., Klump, G., & Winkler, I. (2010). Probability dependence and functional separation of the object-related and mismatch negativity event-related potential components. Neuroimage, 50(1), 285-290.

Bizley, J. K., & Cohen, Y. E. (2013). The what, where and how of auditory-object perception. Nature Reviews Neuroscience, 14(10), 693-707.

Bregman, A. S. (1994). Auditory scene analysis: The perceptual organization of sound. MIT press.

Čeponien, R., Kushnerenko, E., Fellman, V., Renlund, M., Suominen, K., & Näätänen, R. (2002). Event-related potential features indexing central auditory discrimination by newborns. Cognitive Brain Research, 13(1), 101-113.

Čeponienė, R., Lepistö, T., Soininen, M., Aronen, E., Alku, P., & Näätänen, R. (2004). Event‐related potentials associated with sound discrimination versus novelty detection in children. Psychophysiology, 41(1), 130-141.

Coull, J. T. (2009). Neural substrates of mounting temporal expectation. PLoS biology, 7(8), e1000166.

Fell, J., & Axmacher, N. (2011). The role of phase synchronization in memory processes. Nature reviews neuroscience, 12(2), 105-118.

Friston, K., & Kiebel, S. (2009). Predictive coding under the free-energy principle. Philosophical transactions of the Royal Society B: Biological sciences, 364(1521), 1211-1221.

Gibson, E. J. (1963). Perceptual learning. Annual review of psychology, 14(1), 29-56.

Háden, G. P., Honing, H., Török, M., & Winkler, I. (2015). Detecting the temporal structure of sound sequences in newborn infants. International Journal of Psychophysiology, 96(1), 23-28.

Hämäläinen, J. A., Lohvansuu, K., Ervast, L., & Leppänen, P. H. (2015). Event-related potentials to tones show differences between children with multiple risk factors for dyslexia and control children before the onset of formal reading instruction. International Journal of Psychophysiology, 95(2), 101-112.
Jääskeläinen, I. P., Ahveninen, J., Andermann, M. L., Belliveau, J. W., Raij, T., & Sams, M. (2011). Short-term plasticity as a neural mechanism supporting memory and attentional functions. Brain research, 1422, 66-81.
Jones, M. R., & Boltz, M. (1989). Dynamic attending and responses to time. Psychological review, 96(3), 459.
Kidd Jr, G., Mason, C. R., Rohtla, T. L., & Deliwala, P. S. (1998). Release from masking due to spatial separation of sources in the identification of nonspeech auditory patterns. The Journal of the Acoustical Society of America, 104(1), 422-431.
Kidd Jr, G., Mason, C. R., Deliwala, P. S., Woods, W. S., & Colburn, H. S. (1994). Reducing informational masking by sound segregation. The Journal of the Acoustical Society of America, 95(6), 3475-3480.
Kotz, S. A., Stockert, A., & Schwartze, M. (2014). Cerebellum, temporal predictability and the updating of a mental model. Philosophical Transactions of the Royal Society B: Biological Sciences, 369(1658), 20130403.
Kuai, S. G., & Kourtzi, Z. (2013). Learning to see, but not discriminate, visual forms is impaired in aging. Psychological science, 24(4), 412-422.
Kushnerenko, E., Ceponiene, R., Balan, P., Fellman, V., Huotilainen, M., & Näätänen, R. (2002). Maturation of the auditory event-related potentials during the first year of life. Neuroreport, 13(1), 47-51.
Kushnerenko, E. V., Van den Bergh, B. R., & Winkler, I. (2013). Separating acoustic deviance from novelty during the first year of life: a review of event-related potential evidence. Frontiers in psychology, 4, 595.
Li, Q., Liu, G., Wei, D., Guo, J., Yuan, G., & Wu, S. (2019). The spatiotemporal pattern of pure tone processing: a single-trial EEG-fMRI study. Neuroimage, 187, 184-191.
Mayhew, S. D., Dirckx, S. G., Niazy, R. K., Iannetti, G. D., & Wise, R. G. (2010). EEG signatures of auditory activity correlate with simultaneously recorded fMRI responses in humans. Neuroimage, 49(1), 849-864.
Maris, E., & Oostenveld, R. (2007). Nonparametric statistical testing of EEG-and MEG-data. Journal of neuroscience methods, 164(1), 177-190.
McDermott, J. H., Schemitsch, M., & Simoncelli, E. P. (2013). Summary statistics in auditory perception. Nature neuroscience, 16(4), 493-498.
Neubert, C. R., Förstel, A. P., Debener, S., & Bendixen, A. (2021). Predictability-Based Source Segregation and Sensory Deviance Detection in Auditory Aging. Frontiers in Human Neuroscience, 650.
O'Reilly, C., Larson, E., Richards, J. E., & Elsabbagh, M. (2021). Structural templates for imaging EEG cortical sources in infants. Neuroimage, 227, 117682.
O'Sullivan, J. A., Shamma, S. A., & Lalor, E. C. (2015). Evidence for neural computations of temporal coherence in an auditory scene and their enhancement during active listening. Journal of Neuroscience, 35(18), 7256-7263.
Novitski, N., Huotilainen, M., Tervaniemi, M., Näätänen, R., & Fellman, V. (2007). Neonatal frequency discrimination in 250–4000-Hz range: Electrophysiological evidence. Clinical Neurophysiology, 118(2), 412-419.

Paavilainen, P. (2013). The mismatch-negativity (MMN) component of the auditory event-related potential to violations of abstract regularities: a review. International journal of psychophysiology, 88(2), 109-123.
Parviainen, T., Helenius, P., & Salmelin, R. (2019). Children show hemispheric differences in the basic auditory response properties. Human Brain Mapping, 40(9), 2699-2710.
Pearce, M. T. (2005). The construction and evaluation of statistical models of melodic structure in music perception and composition (Doctoral dissertation, City University London).
Pearce, M. T., Ruiz, M. H., Kapasi, S., Wiggins, G. A., & Bhattacharya, J. (2010). Unsupervised statistical learning underpins computational, behavioural, and neural manifestations of musical expectation. NeuroImage, 50(1), 302-313.
Pearce, M. T., & Wiggins, G. A. (2006). Expectation in melody: The influence of context and learning. Music Perception, 23(5), 377-405.
Reed, D. K., Chait, M., Tóth, B., Winkler, I., & Shinn-Cunningham, B. (2020). Spatial cues can support auditory figure-ground segregation. The Journal of the Acoustical Society of America, 147(6), 3814-3818.
Rubin, J., Ulanovsky, N., Nelken, I., & Tishby, N. (2016). The representation of prediction error in auditory cortex. PLoS computational biology, 12(8), e1005058.
Ruhnau, P., Herrmann, B., Maess, B., & Schröger, E. (2011). Maturation of obligatory auditory responses and their neural sources: evidence from EEG and MEG. Neuroimage, 58(2), 630-639.
Saffran, J. R., Johnson, E. K., Aslin, R. N., & Newport, E. L. (1999). Statistical learning of tone sequences by human infants and adults. Cognition, 70(1), 27-52.
Shamma, S. A., Elhilali, M., & Micheyl, C. (2011). Temporal coherence and attention in auditory scene analysis. Trends in neurosciences, 34(3), 114-123.
Shinn-Cunningham, B. G. (2008). Object-based auditory and visual attention. Trends in cognitive sciences, 12(5), 182-186.
Shinn-Cunningham, B. G., Best, V., & Lee, A. K. (2017). The auditory system at the cocktail party.
Slade, K., Plack, C. J., & Nuttall, H. E. (2020). The effects of age-related hearing loss on the brain and cognitive function. Trends in Neurosciences, 43(10), 810-821.
Snyder, J. S., & Alain, C. (2007). Toward a neurophysiological theory of auditory stream segregation. Psychological bulletin, 133(5), 780.
Sohoglu, E., & Chait, M. (2016). Detecting and representing predictable structure during auditory scene analysis. Elife, 5, e19113.
Southwell, R., Baumann, A., Gal, C., Barascud, N., Friston, K., & Chait, M. (2017). Is predictability salient? A study of attentional capture by auditory patterns. Philosophical Transactions of the Royal Society B: Biological Sciences, 372(1714), 20160105.
(((EZ AZ? 3.4-nél)))
Southwell, R., & Chait, M. (2018). Enhanced deviant responses in patterned relative to random sound sequences. Cortex, 109, 92-103.
Stam, C. J., Nolte, G., & Daffertshofer, A. (2007). Phase lag index: assessment of functional connectivity from multi channel EEG and MEG with diminished bias from common sources. Human brain mapping, 28(11), 1178-1193.
Stefanics, G., Hangya, B., Hernádi, I., Winkler, I., Lakatos, P., & Ulbert, I. (2010). Phase entrainment of human delta oscillations can mediate the effects of expectation on reaction speed. Journal of Neuroscience, 30(41), 13578-13585.

Teki, S., Chait, M., Kumar, S., von Kriegstein, K., & Griffiths, T. D. (2011). Brain bases for auditory stimulus-driven figure–ground segregation. Journal of Neuroscience, 31(1), 164-171.
Tóth, B., Kocsis, Z., Háden, G. P., Szerafin, Á., Shinn-Cunningham, B. G., & Winkler, I. (2016). EEG signatures accompanying auditory figure-ground segregation. Neuroimage, 141, 108-119.
Van den Heuvel, M. I., Otte, R. A., Braeken, M. A., Winkler, I., Kushnerenko, E., & Van den Bergh, B. R. (2015). Differences between human auditory event-related potentials (AERPs) measured at 2 and 4 months after birth. International Journal of Psychophysiology, 97(1), 75-83.
Winkler, I., Denham, S. L., & Nelken, I. (2009). Modeling the auditory scene: predictive regularity representations and perceptual objects. Trends in cognitive sciences, 13(12), 532-540.
Zhang, J., & Kourtzi, Z. (2010). Learning-dependent plasticity with and without training in the human brain. Proceedings of the National Academy of Sciences, 107(30), 13503-13508.